

Formation of cobalt nanoparticle dispersions in the presence of polysiloxane block copolymers

M. Rutnakornpituk^a, M.S. Thompson^a, L.A. Harris^a, K.E. Farmer^a, A.R. Esker^a, J.S. Riffle^{a,*}, J. Connolly^b, T.G. St. Pierre^b

^aDepartment of Chemistry, Virginia Polytechnic Institute and State University, Mail Code 0212, Blacksburg, VA 24061-5976, USA

^bDepartment of Physics, The University of Western Australia, Nedlands, Perth, WA 6907, Australia

Received 27 September 2001; received in revised form 4 December 2001; accepted 6 December 2001

Abstract

Stable suspensions of superparamagnetic cobalt nanoparticles have been prepared in poly(dimethylsiloxane) (PDMS) carrier fluids in the presence of poly[dimethylsiloxane-*b*-(3-cyanopropyl)methylsiloxane-*b*-dimethylsiloxane] (PDMS–PCPMS–PDMS) triblock copolymers as steric stabilizers. A series of the polysiloxane triblock copolymers with systematically varied molecular weights were prepared via anionic polymerization using LiOH as an initiator. These copolymers formed micelles in toluene and served as ‘nanoreactors’ for thermal decomposition of the Co₂(CO)₈ precursor. The nitrile groups on the PCPMS central blocks are thought to adsorb onto the particle surface, while the PDMS endblocks protrude into the reaction medium to provide steric stability. The particle size can be controlled by adjusting the cobalt to copolymer ratio. TEM shows non-aggregated cobalt nanoparticles with narrow size distributions which are evenly surrounded with copolymer sheaths. However, some degree of surface oxidation was observed over time, resulting in a decrease in magnetic susceptibility. © 2002 Published by Elsevier Science Ltd.

Keywords: Superparamagnetic; Nanoparticles; Poly(dimethylsiloxane)

1. Introduction

Thermolysis of cobalt carbonyls to form superparamagnetic cobalt nanoparticle clusters has been studied and documented over many years [1–6]. The progressive conversion of Co₂(CO)₈ to Co₄(CO)₁₂, then to metallic cobalt, both in toluene and in the solid state, has been investigated with FTIR to monitor changes in carbon monoxide structure and its disappearance [4]. In recent years, efforts have focused on preparing cobalt particles with narrow size distributions and on preparing close-packed cobalt nanocrystals [5–9]. Self-assembled cobalt nanocrystal arrays with an average particle size of 9 nm diameter were reported from thermolysis of Co₂(CO)₈ in toluene using Na(AOT) as a stabilizer [5,6]. In addition, reduction of CoCl₂ with NaBH₄ in the presence of AOT [7] or using superhydrides in the presence of oleic acid [8] also produced cobalt nanocrystals. Another successful approach developed recently has been to form cobalt nanoparticles in amphiphilic block copolymer micelles [9,10]. It is thought that Co₂(CO)₈ disperses in these reactions, then thermally

decomposes to form nanoparticles inside the micelle cores, whereas the micelle coronas prevent nanoparticle aggregation.

We have previously demonstrated that nanophase separated poly[dimethylsiloxane-*b*-(3-cyanopropyl)methylsiloxane-*b*-dimethylsiloxane] (PDMS–PCPMS–PDMS) triblock polymers can be effective steric dispersion stabilizers for colloidal cobalt particles formed via thermolysis of Co₂(CO)₈ in toluene [11,12]. The central nitrile-functional blocks coordinate with the cobalt surface as a so-called ‘anchor’ block and the poly(dimethylsiloxane) ‘tail’ blocks extend into the toluene to maintain the dispersion. Our motivation for studying this reaction is to prepare well-defined cobalt metal dispersions in poly(dimethylsiloxane) fluids to serve as magnetic nontoxic biomedical materials, particularly for treating retinal detachments [13]. A copolymer having block lengths (15,000 g mol⁻¹ PDMS)–(2000 g mol⁻¹ PCPMS)–(15,000 g mol⁻¹ PDMS) forms transparent solutions when blended into a 2000 g mol⁻¹ *M_n* poly(dimethylsiloxane) fluid. Thus, when this block copolymer was used to stabilize cobalt nanoparticles, the cobalt–toluene dispersions could be transferred from the toluene preparation solvent to the 2000 g mol⁻¹ poly(dimethylsiloxane) carrier fluid [11]. These dispersions are

* Corresponding author. Tel.: +1-540-231-8214; fax: +1-540-231-8517.
E-mail address: judyriffle@aol.com (J.S. Riffle).

stable over at least a year under ambient conditions, and exhibit no signs of precipitation. It should be noted, however, that the oxidative stability of these cobalt nanoparticles needs improvement, and this aspect is central to much of our ongoing work.

The present paper describes cobalt carbonyl thermolysis reactions in the presence of block copolymer micelles as reaction sites. Relationships between the block lengths in the copolymer stabilizers, the reactant concentrations, dispersion stability, and the resultant cobalt nanoparticle size have been investigated. It is clear that some control over the metal nanoparticle size is possible by adjusting the ratio of the dicobalt octacarbonyl precursor to the copolymer.

2. Experimental

2.1. Materials

Tetramethylcyclotetrasiloxane (D_4H , the Dow-Corning Corp.) and octamethylcyclotetrasiloxane (D_4 , the Dow-Corning Corp.) were dried over calcium hydride overnight and fractionally distilled prior to use. A Pt^0 [1,3-divinyl-1,1,3,3-tetramethyldisiloxane] $_{1.5}$ complex in xylene (2.1–2.4 wt% Pt) catalyst (Gelest, Inc.) was used as received. Triflic acid (Aldrich) was used as received. Allyl cyanide (98%, Aldrich) was dried over 4 Å molecular sieves for at least 2 days, then distilled under argon. LiOH (Aldrich) was ground in a dry box and stored under argon until used. Toluene (Fisher) and dichloromethane (Baxter) were washed twice with concentrated sulfuric acid, and then neutralized with water. They were then dried with anhydrous magnesium sulfate, toluene was stirred over calcium hydride, and dichloromethane was stirred over phosphorus pentoxide, then each was distilled prior to use. Hexamethylcyclotrisiloxane (D_3 , Gelest, Inc.) was purified by stirring over calcium hydride at 80 °C overnight, then fractionally distilled under argon into a pre-dried and pre-weighed flask. Tetrahydrofuran (99.5%, E.M. Sciences) was dried over calcium hydride overnight and then refluxed over sodium with benzophenone until the solution was deep purple and distilled prior to use. Hexamethyldisiloxane (99%, Gelest, Inc.), used as an endcapping reagent for PDMS carrier fluids, was fractionally distilled prior to use. Trimethylchlorosilane (Gelest, Inc.), used as an endcapping reagent for the triblock copolymers, was fractionally distilled prior to use. $Co_2(CO)_8$ (Alpha Easar) stabilized with 1–5% hexane was stored under argon without further purification.

2.2. Synthesis

Synthetic methods for preparing the monomers and block copolymers discussed in this paper have been described previously [11]. Thus, only an exemplary copolymer synthesis will be included herein.

2.2.1. Synthesis of poly[*dimethylsiloxane-b-(3-cyanopropyl)methylsiloxane-b-dimethylsiloxane*] triblock copolymers (PDMS–PCPMS–PDMS) with controlled block lengths

A procedure for preparing a copolymer with a targeted number average molecular weight comprised of 5000 g mol⁻¹ PDMS and 5000 g mol⁻¹ PCPMS blocks is provided. Copolymers with other block lengths were prepared in a similar manner but with different ratios of lithium hydroxide to D_4CN to tailor the molecular weight of the central block, and with different amounts of D_3 relative to the central block to tailor the endblock molecular weights. One other variation in these syntheses was that tetrahydrofuran was utilized as the reaction rate promoter in cases of short poly(dimethylsiloxane) endblocks and tetraethylene glycol dimethylether (TEGDME) was often utilized for longer endblocks. TEGDME afforded faster reaction rates which were useful for preparing higher molecular weight blocks, but this promoter was more difficult to remove quantitatively in the copolymer recovery step. The first part of the copolymer synthesis involves the preparation of controlled molecular weight PCPMS oligomers with terminal lithium siloxanates. D_4CN (21.8 g) and 0.1552 g (0.0065 mol) lithium hydroxide were charged to a clean, dry 500-ml round-bottom flask equipped with a mechanical stirrer and nitrogen purge. The mixture was stirred at 140 °C for a minimum of 48 h to reach thermodynamic equilibrium. The approach to equilibrium was monitored by GPC using samples which had been neutralized with acetic acid. The ratio of cyclics to linear species at equilibrium was 27 wt% small cyclics and 73 wt% linear chains. After equilibrium was achieved, 100 ml of dichloromethane were added to the macroinitiator via cannula. An 80 ml aliquot of a D_3 -dichloromethane solution (0.434 g D_3 per ml) was added along with 20 ml THF as a reaction rate promoter. Twenty ml of promoter (either THF or TEGDME) per 21.8 g D_4CN were added to all block copolymer reactions irrespective of the block molecular weights. Another 60 ml of dichloromethane was added to bring the reaction volume to ≈260 ml and to obtain a clear solution. The disappearance of the D_3 protons at 0.14 ppm from TMS was monitored by ¹H NMR. The reaction was allowed to proceed at room temperature for 7 days (85% monomer conversion). The triblock copolymer was terminated with an excess of trimethylchlorosilane (0.822 ml) via syringe and stirred for approximately 30 min. The solution clouds upon termination due to precipitation of LiCl. The excess trimethylchlorosilane and the dichloromethane solvent were removed under reduced pressure. The viscous copolymer was diluted with chloroform and washed repeatedly with water to remove the lithium chloride. The copolymer–chloroform solution was precipitated into methanol to remove nitrile containing siloxane cyclics (from the central block equilibration step) and the THF promoter. The methanol phase was decanted, then the polymer was dried at 80 °C under vacuum overnight. It should be noted that the

precipitation procedure into methanol had to be repeated several times when TEGDME was used as the reaction promoter. The block molecular weights and the total molecular weights of the triblock copolymers after purification were established using a combination of titration and NMR measurements. Molecular weights of the copolymer blocks described in this procedure were (5530 g mol⁻¹ PDMS)–(5000 g mol⁻¹ PCPMS)–(5530 g mol⁻¹ PDMS).

2.2.2. Synthesis of a superparamagnetic cobalt fluid stabilized with a (5530 g mol⁻¹ PDMS)–(5000 g mol⁻¹ PCPMS)–(5530 g mol⁻¹ PDMS) block copolymer in toluene

The reaction apparatus consisting of a 500-ml three-neck round-bottom flask equipped with a mechanical stirrer having a vacuum tight adapter, condenser and argon purge was oven dried and assembled under argon. This was placed in a temperature controlled silicone oil heating bath over a hot plate (without magnetic stirrer). Twenty ml toluene and 1.0 g of the copolymer were charged with stirring. After the copolymer dissolved, 1.0 g of bright orange dicobalt octacarbonyl was added and dissolved at room temperature. Immediately upon adding the dicobalt octacarbonyl, a greenish-brown gas fills the flask and refluxes. The oil bath thermocouple was set to 45 °C and the reaction was allowed to slowly warm, then the 45 °C oil bath temperature was maintained for 45 min. Persistent foaming occurred during this stage which subsided toward the end of the 45 min period. The reaction temperature was raised to 120 °C to yield a greenish-brown solution. Foaming again commenced soon after reaching the desired temperature. The reaction was allowed to proceed at 120 °C for 2 h. Upon cooling, a stable dispersion of cobalt nanoparticles in the copolymer–toluene medium resulted.

2.2.3. Preparation of stable cobalt nanoparticle dispersions in PDMS carrier fluids

Dispersions with specified cobalt concentrations were prepared in a 2000 g mol⁻¹ M_n poly(dimethylsiloxane) carrier fluid by first transferring an aliquot of the cobalt dispersion in toluene to a vial, diluting the sample with the appropriate carrier fluid, then removing toluene under reduced pressure. Careful attention should be given to exclude oxygen during this process to avoid cobalt particle surface oxidation and preserve the saturation magnetization of these fluids. Quantitative toluene removal was confirmed by the disappearance of the aromatic C–H stretches in the FTIR at ≈ 3000 – 3100 cm⁻¹.

2.2.4. Synthesis of a 2000 g mol⁻¹ M_n poly(dimethylsiloxane) carrier fluid (PDMS)

Two hundred ml of octamethylcyclotetrasiloxane (D₄) and 20 ml of hexamethyldisiloxane endcapping reagent were charged to a 500 ml flame-dried, argon filled, round bottom flask containing a magnetic stir bar and

capped with a septum. The reaction flask was placed in an oil bath at 65 °C. Triflic acid (0.2 ml) was slowly added and the reaction mixture was maintained at the 65 °C temperature for 3 days until thermodynamic equilibrium was achieved. This reaction condition was established by observing the equilibrium peaks in gel permeation chromatography. Following the reaction, 60 ml of ethyl ether was added into the solution and it was then washed with water six times to neutralize the mixture. The equilibrium concentration of D₄ monomer and water were removed under reduced pressure at 120 °C overnight.

2.3. Characterization

The copolymer solutions for surface tension and dynamic light scattering measurements were prepared in toluene at least 24 h before the measurements to allow sufficient time for complete dissolution. Copolymer solutions in toluene with concentrations of 0.1 g l⁻¹ or higher were syringed through 0.1 μ m pore filters and those with lower concentrations were syringed through 0.02 μ m pore filters prior to surface tension and light scattering measurements. Surface tension measurements of the copolymer solutions in toluene were conducted at ≈ 26 °C using a platinum Wilhelmy plate apparatus in combination with a Langmuir–Blodgett trough (KSV 2000, KSV Instruments, Inc., Finland). Surface tensions were calculated using the relationship $\Delta F = \gamma P \cos \theta$ where ΔF is the difference in weight between the wet plate and the wet plate in contact with the solution, γ is the surface tension, P is the perimeter of the plate and the contact angle θ is assumed to be 0°. Dynamic light scattering measurements were obtained using a Protein Solutions DynaPro-80ITC instrument at 25 °C. The translational diffusion coefficients (D_T) for the molecules in the solutions were calculated from the scattered light intensities. Hydrodynamic radii (R_h) were derived from D_T using the Stokes–Einstein equation. The reported hydrodynamic radii are the average of at least ten measurements. FTIR spectra were obtained using a Nicolet Impact 400 FTIR spectrometer with the samples run neat between salt plates. Transmission electron micrographs were obtained using a Phillips 420T TEM run at 100 kV. The TEM samples of the cobalt dispersions in toluene or poly(dimethylsiloxane) carrier fluids were prepared by diluting the dispersions with additional toluene to obtain the color of ‘weak tea’. The solutions were cast onto a carbon-coated grid and the toluene was evaporated. Selected TEM images were analyzed using a fast Fourier transform (FFT) of a 128 pixel square region within the image. The intensities of each pixel of the FFT images were radially averaged. In this process, the pixels of the transformed image were grouped according to their distance from the center of the image and the intensities of each group summed to give a total intensity for each length scale.

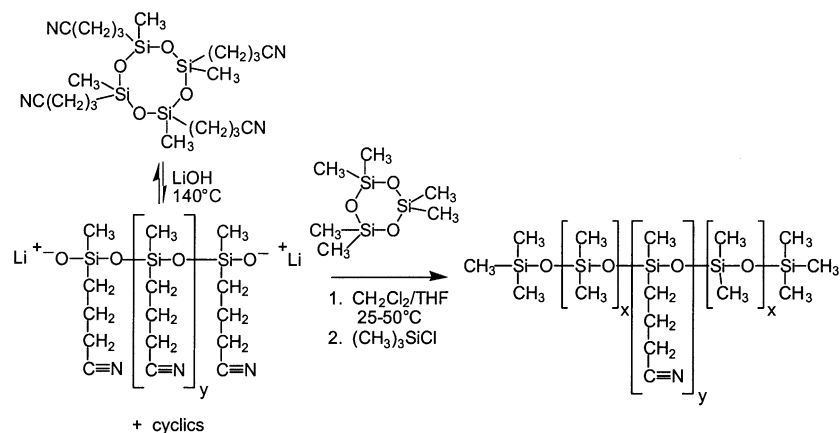


Fig. 1. Synthesis of PDMS-PCPMS-PDMS triblock copolymers.

2.4. Magnetic properties

Four cobalt nanoparticle dispersions stabilized with a (15,000 g mol⁻¹ PDMS)–(2000 g mol⁻¹ PCPMS)–(15,000 g mol⁻¹ PDMS) copolymer in a 2000 *M_n* PDMS carrier fluid with Co concentrations between 1.6 and 4.1% were flame sealed into 4 mm diameter glass tubes under an argon atmosphere. An additional four samples with concentrations between 1.9 and 6.1% were sealed in glass tubes with polycarbonate lids without excluding air from the volume of gas above the liquid. The concentration of each sample is given in Table 1.

Magnetic properties of the cobalt dispersions were measured using a SQUID based magnetic susceptometer (Quantum Designs MPMS-7). Magnetic hysteresis loops were measured at 5 K after cooling the sample from 220 K in a zero or 70 kOe field. The magnetic moment of the sample was measured in fields from –70 to 70 kOe. The time interval between initial and final hysteresis loop measurements of samples 5–8 was 180 days, with an additional measurement taken at an intermediate time point. The time interval between initial and final hysteresis loop measurements of samples 1–4 varied from 40 to 90 days.

3. Results and discussion

3.1. PDMS-PCPMS-PDMS micellar solutions in toluene

One goal has been to investigate cobalt nanoparticle

formation in reactions wherein dicobalt octacarbonyl can diffuse into the core of block copolymer micelles, and then thermally eliminate carbon monoxide inside the core. The electron pairs on the nitrile nitrogens of the PCPMS stabilizer central block are believed to interact with the cobalt nanoparticle surfaces to anchor the stabilizer to the particles (Fig. 1). It is reasoned that controlled micelle ‘nanoreactor’ size and structure may enable better control over metal particle size, and may also provide improved copolymer coatings. The stabilizer coating quality is anticipated to be important for minimizing any toxicity issues *in vivo* in potential biomedical applications. Thus, understanding the solution structures of the block copolymers in the toluene reaction solvent is a key issue.

Toluene is a good solvent for PDMS but a poor solvent for PCPMS, particularly for higher molecular weight PCPMS oligomers. For example, 3 g l⁻¹ of an 8000 g mol⁻¹ *M_n* PCPMS in toluene is the maximum concentration which is soluble. Only 1 g l⁻¹ of a 24,000 g mol⁻¹ *M_n* PCPMS is soluble, whereas 37,000 g mol⁻¹ PCPMS is essentially insoluble in toluene. The PDMS-PCPMS-PDMS block copolymers form micellar solutions in toluene where the PCPMS is concentrated in the micelle cores and PDMS protrudes outward into toluene to form the micelle coronas.

Surface tensions of block copolymer solutions in toluene as well as dynamic light scattering suggest these solutions contain block copolymer micelles. At sufficiently low copolymer concentrations, surface tensions approached the

Table 1

Sample codes and cobalt concentrations of dispersions used for magnetic measurements. Cobalt particles were stabilized with a (15,000 g mol⁻¹ PDMS)–(2000 g mol⁻¹ PCPMS)–(15,000 g mol⁻¹ PDMS) copolymer and dispersed in a 2000 *M_n* PDMS carrier fluid

Air-exposed solutions		Non-air-exposed solutions	
Sample code	Concentration (% Co)	Sample code	Concentration (% Co)
1	6.7	5	4.1
2	4.9	6	3.2
3	3.2	7	2.3
4	1.9	8	1.6

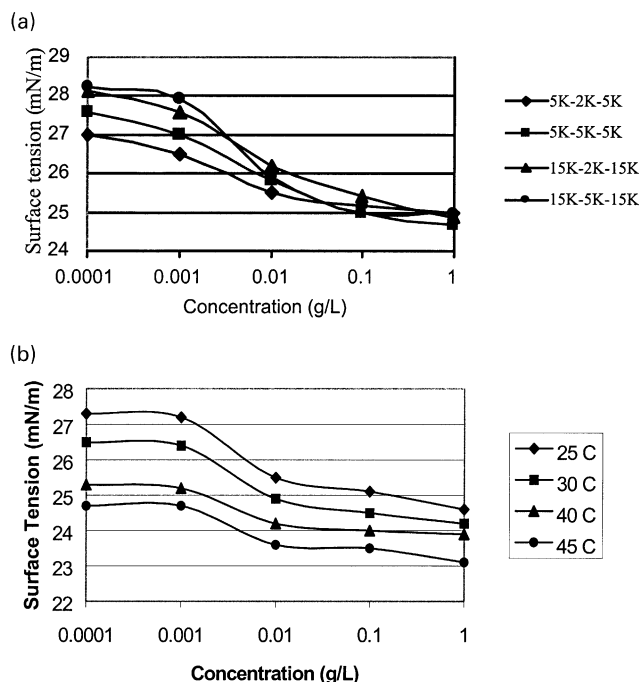


Fig. 2. (a) Surface tensions of solutions of the PDMS–PCPMS–PDMS triblock copolymers in toluene at 26 °C showing a CMC of 0.01 g l⁻¹. (b) Surface tensions of solutions of (15,000 g mol⁻¹ PDMS)–(2000 g mol⁻¹ PCPMS)–(15,000 g mol⁻¹ PDMS) copolymers in toluene at various temperatures.

value for pure toluene (Fig. 2(a)). The surface tension at the lowest concentration (0.0001 g l⁻¹) is close to the reported value of pure toluene at the same temperature (28.5 mN m⁻¹) [14]. PCPMS center blocks in these materials tend to migrate to the solution surface due to their poor solubilities in toluene. Once the copolymer concentrations were increased, surface tensions dropped between ≈ 0.001 and 0.01 g l⁻¹, then leveled off for higher concentrations. This result suggests saturation of the solution surfaces by the copolymers with critical micelle concentrations (CMC) of about 0.01–0.1 g l⁻¹. Further increases in concentration above the CMC lead to micellar solutions.

Surface tension measurements of (15,000 g mol⁻¹ PDMS)–(2000 g mol⁻¹ PCPMS)–(15,000 g mol⁻¹ PDMS) copolymer solutions in toluene were also conducted up to 45 °C

Table 2

Hydrodynamic radii measured by dynamic light scattering demonstrate large increases in radii at the CMC, consistent with formation of micellar structures

Concentration (g l ⁻¹)	Hydrodynamic radii (R_h) of PDMS–PCPMS–PDMS (nm)			
	5K–2K–5K	5K–5K–5K	15K–2K–15K	15K–5K–15K
5	15.35 ± 0.08	21.35 ± 0.61	11.78 ± 0.62	26.70 ± 0.08
1	13.54 ± 0.35	20.43 ± 0.06	11.63 ± 0.73	21.77 ± 0.02
0.5	12.80 ± 0.16	18.61 ± 0.09	11.86 ± 0.49	21.33 ± 0.15
0.1	12.02 ± 1.11	15.45 ± 2.28	11.72 ± 0.65	6.99 ± 0.14
0.01	11.47 ± 0.61	12.19 ± 0.86	2.8 ± 0.40	5.25 ± 0.38
0.001	3.38 ± 1.50	4.13 ± 1.03	N/A	4.38 ± 0.05

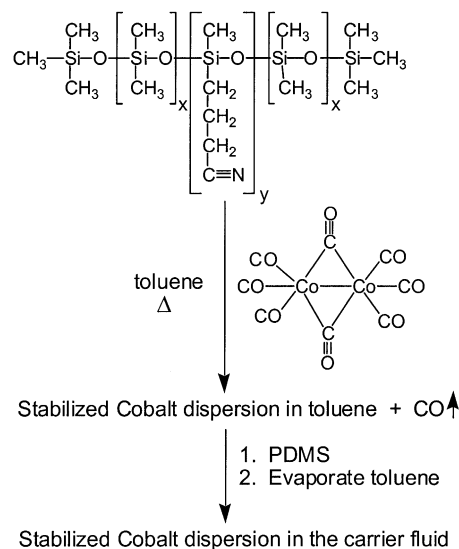


Fig. 3. Preparation of a cobalt nanoparticle dispersion in toluene.

to determine whether the CMC's changed substantially as a function of temperature (Fig. 2(b)).

The 45 °C case was of particular interest because this was the temperature used in the initial stages of the cobalt nanoparticle dispersion syntheses. As expected [15,16], the surface tensions were consistently lower as temperature increased. However, the drop in surface tension caused by the copolymers occurred over a rather broad concentration region, and no differences in the CMC's could be distinguished (0.01–0.1 g l⁻¹ from 25 to 45 °C). This observation suggests that if the cobalt dispersions are prepared at 45 °C or higher with a PDMS–PCPMS–PDMS copolymer concentration higher than the CMC, it is reasonable to assume that micelles are present in the reaction solutions.

Dynamic light scattering further supports the micellar structures in toluene. When copolymer solutions containing small PDMS blocks (5000 g mol⁻¹) were examined, hydrodynamic radii increased from an average of ≈ 3 –4 nm at 0.001 g l⁻¹ (indicative of single molecules) to ≈ 11 –12 nm at 0.01 g l⁻¹ (indicative of aggregates of molecules) (Table 2). This change occurred at somewhat higher concentrations when the PDMS block length was increased to 15,000 g mol⁻¹. The transitions from molecular to aggregate sizes observed by light scattering occurred in the

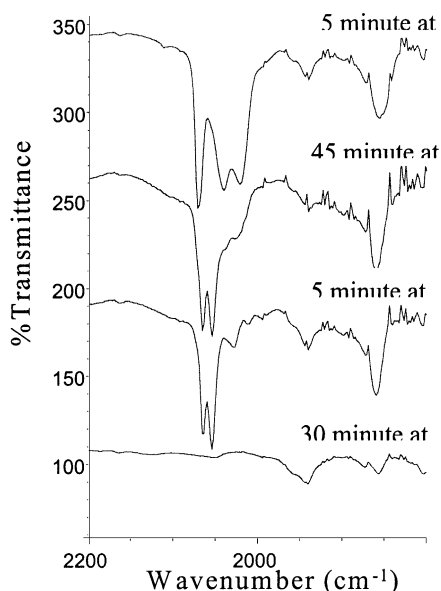


Fig. 4. FTIR spectra of a cobalt dispersion using 1 g $\text{Co}_2(\text{CO})_8$ and 1 g of a $(15,000 \text{ g mol}^{-1} \text{ PDMS})-(2000 \text{ g mol}^{-1} \text{ PCPMS})-(15,000 \text{ g mol}^{-1} \text{ PDMS})$ copolymer in 20 ml toluene at different stages.

concentration ranges where CMC's were observed in the surface tension measurements.

3.2. Synthesis of cobalt nanoparticles by thermolysis of dicobalt octacarbonyl in the micellar copolymer solutions

The cobalt dispersion reactions were conducted in copolymer–toluene solutions (Fig. 3) at copolymer concentrations ranging from 10 to 150 g l^{-1} , which is much more concentrated than the solutions investigated by light scattering. Based on our understanding of the structures of the copolymer–toluene solutions, it is reasonable to assume that copolymer micelles as well as micelle aggregates exist under these conditions.

The progress of a series of reactions was studied by FTIR coupled with TEM to monitor the transformation of paramagnetic species into superparamagnetic particles. These studies were conducted with low (0.2 g), medium (1.0 g) and high (3.2 g) concentrations of $\text{Co}_2(\text{CO})_8$ and 1.0 g of a $(15,000 \text{ g mol}^{-1} \text{ PDMS})-(2000 \text{ g mol}^{-1} \text{ PCPMS})-(15,000 \text{ g mol}^{-1} \text{ PDMS})$ copolymer in 20 ml of toluene. The reactions were first heated to 45°C where the reactions began, and were maintained at that temperature for 45 min. Significant foaming initially occurred in this stage due to evolution of carbon monoxide, which subsided toward the end of the 45 min. The carbon monoxide region around 2000 cm^{-1} in the FTIR (Fig. 4) initially showed three absorbance bands at 2020, 2050 and 2070 cm^{-1} attributed to terminal CO and a peak at 1860 cm^{-1} due to bridging CO in $\text{Co}_2(\text{CO})_8$ [4]. By the end of the 45 min at 45°C , the absorbance at 2020 and 2050 cm^{-1} had greatly decreased suggesting a large reduction in starting material, and two sharp peaks at 2055 and 2065 cm^{-1} appeared,

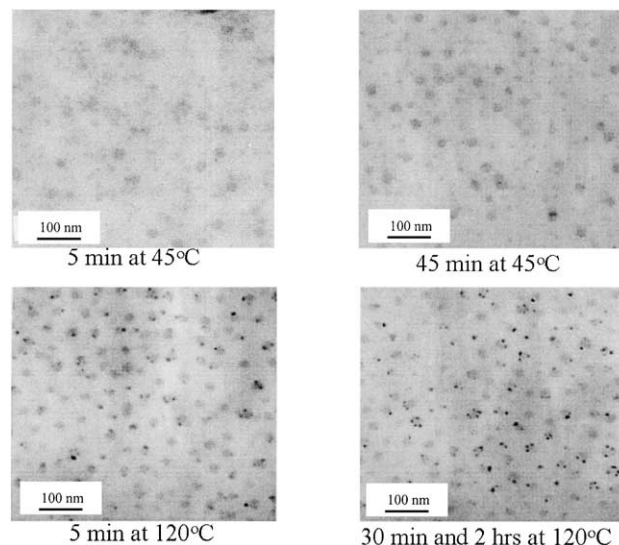


Fig. 5. Transmission electron micrographs of cobalt dispersions using 0.2 g $\text{Co}_2(\text{CO})_8$ and 1 g of a $(15,000 \text{ g mol}^{-1} \text{ PDMS})-(2000 \text{ g mol}^{-1} \text{ PCPMS})-(15,000 \text{ g mol}^{-1} \text{ PDMS})$ copolymer in 20 ml toluene at different stages.

which were attributed to $\text{Co}_4(\text{CO})_{12}$. The temperature was then raised to 120°C where the toluene refluxed and foaming caused by additional CO evolution commenced again. After 30 min at this temperature, all CO had disappeared as indicated by its absence in the FTIR spectra.

At all of the cobalt carbonyl to copolymer ratios investigated, TEM photomicrographs from aliquots taken in the early reaction stages (5 min at 45°C) showed clusters of particles with aggregate sizes 20–50 nm in diameter (Figs. 5–7). These clusters were thought to be micelle aggregates essentially stained with $\text{Co}_2(\text{CO})_8$. By contrast, no features were observable in the TEM photomicrographs from analogous copolymer solutions without $\text{Co}_2(\text{CO})_8$. After 45 min reaction at 45°C , the particle aggregates were smaller and appeared denser as evidenced by darkened regions. A significant portion of the $\text{Co}_2(\text{CO})_8$ may have been converted to compounds such as $\text{Co}_4(\text{CO})_{12}$ by this stage. The FTIR showed strong peaks at 2055 and 2065 cm^{-1} attributed to CO groups in $\text{Co}_4(\text{CO})_{12}$, the product from the first step of the solution decomposition of $\text{Co}_2(\text{CO})_8$ [4]. It was reasoned that $\text{Co}_2(\text{CO})_8$ was at least partly decomposed and cobalt paramagnetic species had begun to interact with their counterparts in adjacent atoms.

The temperature was subsequently raised to 120°C to further thermolyze the cobalt carbonyl mixtures. After 5 min at this temperature, foaming again began and the TEM images showed 10–20 nm diameter particles which had further densified over this short period. After 30 min at 120°C , foaming had subsided and all of the CO peaks in the FTIR had disappeared, suggesting that the reactions were complete. In all cases, the average particle sizes after 2 h reaction at 120°C were equal to those after 30 min reaction at the same temperature. However, most

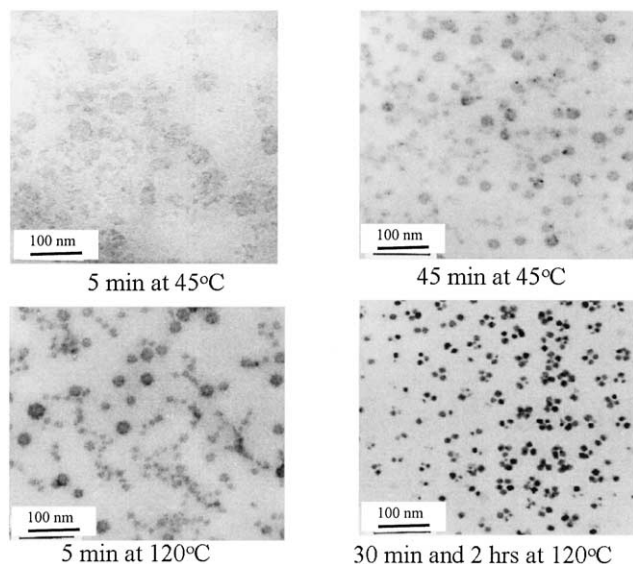


Fig. 6. Transmission electron micrographs of cobalt dispersions using 1.0 g $\text{Co}_2(\text{CO})_8$ and 1 g of a $(15,000 \text{ g mol}^{-1} \text{ PDMS})-(2000 \text{ g mol}^{-1} \text{ PCPMS})-(15,000 \text{ g mol}^{-1} \text{ PDMS})$ copolymer in 20 ml toluene at different stages.

of the reactions were maintained at 120 °C for 2 h to ensure that CO was completely removed.

The reaction products prepared with the low and medium cobalt carbonyl to copolymer ratios were dark, colloidal dispersions without any visible precipitates. The metal particle sizes within each reaction were near monodisperse and each particle was surrounded with a well-defined copolymer sheath (Figs. 5 and 6). It is suggested that the homogeneity of the copolymer coatings surrounding each particle may be a result of forming the metal nanoparticles within the copolymer micelles, as opposed to first forming the particles, then coating them. This issue may be important for the intended biomedical applications of these materials as we strive to develop methodologies which minimize toxicity.

At the higher cobalt carbonyl to copolymer ratio (3.2 g $\text{Co}_2(\text{CO})_8$ to 1 g copolymer), various particle sizes (10, 25 and 45 nm) with some aggregation were observed (Fig. 7). Thus, the upper limit on the initial molar ratio of $\text{Co}_2(\text{CO})_8$ to copolymer appears to be about 1:1 wt/wt in these reactions to ensure that each particle forms within the micelles and that precipitation is avoided. In addition, undesirably large particles formed in these reactions, and assembled into oriented chains at this high cobalt carbonyl/copolymer ratio, resembling the behavior of 'nanoscale magnets' dispersed in the solutions. It was reasoned that dipole-dipole interactions among adjacent magnetically blocked particles had been induced, resulting in particle chain formation.

Interestingly, TEM photomicrographs of the final dispersions formed from the medium concentration cobalt carbonyl/copolymer reactions (1 g cobalt octacarbonyl, 1 g copolymer, 20 ml toluene) showed many particle multiplets consisting of 2–4 small particles, with each particle within the multiplet ≈ 10 nm in diameter, but joined together mostly in triplets and quartets (Fig. 6). Each of the cobalt

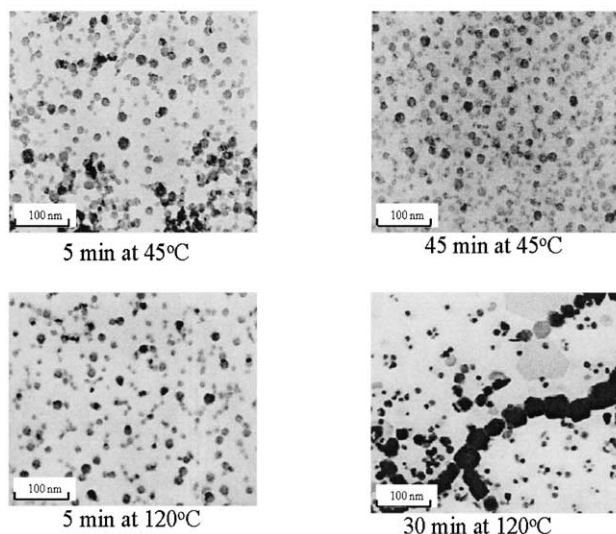


Fig. 7. Transmission electron micrographs of cobalt dispersions using 3.2 g $\text{Co}_2(\text{CO})_8$ and 1 g of a $(15,000 \text{ g mol}^{-1} \text{ PDMS})-(2000 \text{ g mol}^{-1} \text{ PCPMS})-(15,000 \text{ g mol}^{-1} \text{ PDMS})$ copolymer in 20 ml toluene at different stages.

particles within the multiplets was individually surrounded with the copolymer sheath. Although this aspect will require further investigation to be well understood, this may be a result of some aggregation of the micelles in the solution during synthesis. Indeed, the TEM photomicrographs in Fig. 6 suggest the existence of this multiplet structure throughout the reaction stages. Two to four micelles, grouped together, can be observed in the photomicrograph of the reaction after 5 min at 45 °C, and these become smaller and denser in the later stages (Fig. 6).

3.3. The cobalt dispersion reaction in the presence of an external magnetic field

To determine the stage in the synthesis of the cobalt nanoparticle dispersions where the particles became superparamagnetic, a cobalt dispersion was prepared using 1.0 g of $\text{Co}_2(\text{CO})_8$ and 1.0 g of a $(15,000 \text{ g mol}^{-1} \text{ PDMS})-(2000 \text{ g mol}^{-1} \text{ PCPMS})-(15,000 \text{ g mol}^{-1} \text{ PDMS})$ copolymer in 20 ml of toluene in the presence of an external magnetic field (provided by a permanent magnet placed under the reaction vessel). Aliquots from the reaction mixture were removed at various stages and investigated with TEM. After the reaction had proceeded for 45 min at 45 °C (after foaming subsided), no differences between this dispersion and that from an analogous reaction conducted under the normal conditions (no external field) were observed, indicating that the particles had not yet become superparamagnetic. On the other hand, the dispersion after 5 min at 120 °C (foaming had again commenced) manifested a significant difference from the control reaction carried out in the absence of the applied field. Relatively large particles, 20–50 nm in diameter, had formed and were oriented in chains. This suggests that the transition

Table 3
Particle size control studies

Co ₂ (CO) ₈ (g)	Copolymer (g)	Toluene (ml)	Particle diameter (nm)		
			15K–2K–15K	5K–5K–5K	15K–5K–15K
<i>Effect of the ratio of Co₂(CO)₈ to copolymers</i>					
0.2	1	20	6	7	7
0.33	1	20	9	10	9
1.0	1	20	10	10	10
1.8	1	20	Aggregation	Aggregation	Aggregation
3.2	1	20	Aggregation	Aggregation	Aggregation
<i>Effect of amount of toluene in the reaction mixtures</i>					
1	1	20	10	10	10
1	1	60	12	11	10
1	1	100	12	10	10

to superparamagnetic particles occurs soon after the 120 °C temperature is employed. It appears that the external magnetic field induced strong dipole–dipole interactions among the magnetic particles which overcame thermal energy, and resulted in oriented chains which were locked in place even after the external magnet was removed.

3.4. Effects of the Co₂(CO)₈/copolymer ratio on cobalt nanoparticle size

Controlling particle size in the nanoscale regime to obtain cobalt nanoparticles with a narrow size distribution is of particular interest. Due to their nanoscale size, the particles are single magnetic domains and exhibit superparamagnetic behavior. Formation of larger particles is undesirable because this increases the possibility of aggregation via magnetic attractions between particles.

Reactions with five concentrations of Co₂(CO)₈ with each of four copolymers were conducted in 20 ml of toluene (Table 3). The block lengths of the copolymers were controlled to investigate any influences of a low (2000 g mol⁻¹) molecular weight versus a higher molecular weight (5000 g mol⁻¹) anchor block length and also a low (5000 g mol⁻¹) and higher molecular weight (15,000 g mol⁻¹) tail block length. In all cases, the anchor block length was significantly shorter than the tail length since previous work has shown this to be the desirable range for providing good steric stabilization [11–13].

The cobalt particle sizes increased from 6 nm in diameter at the low concentration (0.2 g Co₂(CO)₈ to 1 g of copolymer) to 10 nm diameter at the medium concentration (1.0 g Co₂(CO)₈ to 1 g of copolymer) (Table 3). The 6 nm size was attributed to formation of cobalt nanoparticles in micelle cores where the cores had not been ‘filled up’ with the cobalt carbonyl organometallic precursor. Thus, these early results suggest that some control over particle size in the lower nanoscale regime can be obtained by controlling the cobalt carbonyl to block copolymer ratio. When the cobalt carbonyl to copolymer ratio was increased, the particles were larger up to about 10 nm, then further increases resulted in

precipitates. It seems that once the organometallic precursor concentration was raised high enough to ‘fill up’ the micelle cores, further controlled increases in metal particle size may not be obtainable by this method. No differences in particle sizes were observed as the block lengths of the copolymers were varied in this range.

Dispersions were also investigated with a constant ratio of Co₂(CO)₈ to copolymers but with systematically varied amounts of toluene (Table 3). As expected, cobalt particle size was independent of the concentrations of Co₂(CO)₈ and copolymers in the toluene.

3.5. Formation and characterization of poly(dimethylsiloxane) dispersions

Superparamagnetic cobalt dispersions in low molecular weight PDMS carrier fluids were prepared. A 2000 g mol⁻¹ PDMS carrier fluid was synthesized via an equilibrium reaction of D₄ using triflic acid as a catalyst. The molecular weight was controlled by using one mole of hexamethyldisiloxane endcapping reagent for every mole of polymer to produce non-functional PDMS. It should be noted that the polysiloxane triblock copolymers with long PCPMS central blocks and short PDMS tail blocks (e.g. (5000 g mol⁻¹ PDMS)–(5000 g mol⁻¹ PCPMS)–(5000 g mol⁻¹ PDMS)) have less solubility in the PDMS homopolymer than those with short PCPMS central blocks and long PDMS tails (e.g. (15,000 g mol⁻¹ PDMS)–(2000 g mol⁻¹ PCPMS)–(15,000 g mol⁻¹ PDMS)). This corresponds to the fact that high molecular weight PCPMS is insoluble in low molecular weight PDMS. The cobalt dispersions were prepared using 1.0 g of a (15,000 g mol⁻¹ PDMS)–(2000 g mol⁻¹ PCPMS)–(15,000 g mol⁻¹ PDMS) copolymer and 1.0 g of Co₂(CO)₈ in 20 ml of toluene. Once the reaction was completed (indicated by the disappearance of CO peaks at 2055 and 2065 cm⁻¹ in FTIR), the desired amount of 2000 g mol⁻¹ PDMS carrier fluid was syringed into the dispersion and the toluene was removed under reduced pressure. The disappearance of the aromatic C–H absorbances above 3000 cm⁻¹ in the FTIR suggested that

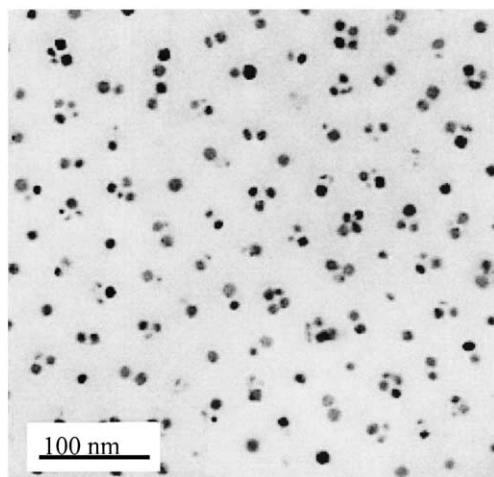


Fig. 8. Transmission electron micrographs of cobalt dispersions in $2000 \text{ g mol}^{-1} M_n$ PDMS carrier fluids.

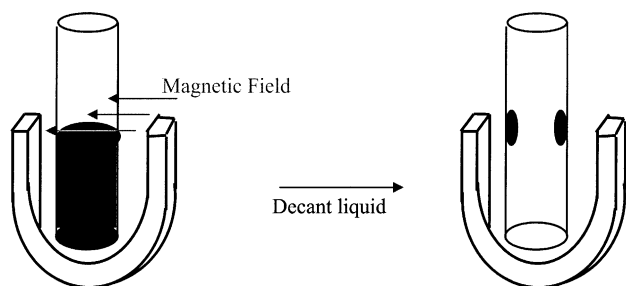


Fig. 9. Magnetic separation of cobalt dispersions using an externally applied magnetic field gradient.

toluene was completely removed. TEM showed that the resultant dispersions had a narrow size distribution comprised of $\approx 10 \text{ nm}$ diameter particles with 2–4 particles per multiplet (Fig. 8).

3.6. Two-dimensional ordering of superparamagnetic cobalt nanoparticles

A magnetic separation was conducted on a stable cobalt dispersion which had been prepared using 1.0 g of a $(15,000 \text{ g mol}^{-1} \text{ PDMS})-(2000 \text{ g mol}^{-1} \text{ PCPMS})-(15,000 \text{ g mol}^{-1} \text{ PDMS})$ copolymer, 1.0 g of $\text{Co}_2(\text{CO})_8$, and 20 ml of toluene. The stable dispersion was placed in a weak magnetic field gradient generated by a horseshoe permanent magnet (Fig. 9). After 24 h , superparamagnetic particles collected in the regions with highest field. Presumably, anti-ferromagnetic cobalt oxides and small particles remained dispersed in the solution. While the magnetic field was maintained in place, the solution was decanted, then the container with the remaining (strongly superparamagnetic) nanoparticles was rinsed with toluene. The nanoparticles which had been separated by the field gradient of the horseshoe magnet redispersed in the toluene.

To prepare the samples for TEM, one drop of the solution was cast onto a carbon-coated grid and the toluene was slowly evaporated at 25°C . The resultant dispersion prepared from the particles which were collected in the weak external field gradient formed an ordered self-assembled cobalt nanoparticle array (Fig. 10). Although some order existed in the original dispersion, the field gradient separation greatly increased the order. Radially averaged FFT plots generated from digitized TEM images showed clear peaks at approximately 43 , 19 and 9 nm (Fig. 11). These three length scales can be attributed to intercluster spacing, cluster size, and particle size, respectively. The self-assembled array is a result of interparticle interactions. However, it is not possible to determine the source of this interaction from the TEM images. It is also not clear whether the clusters observed were present in the fluid phase, or were formed during evaporation of the fluid.

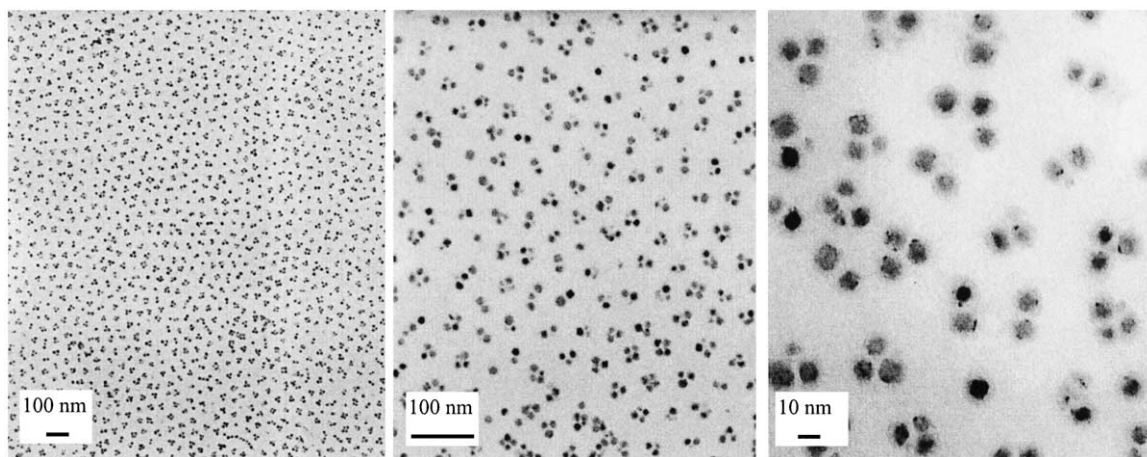


Fig. 10. Self-assembled two-dimensional ordering of magnetic field separated cobalt nanoparticles on a carbon film, from a reaction using 1 g $\text{Co}_2(\text{CO})_8$ and 1 g of a $(15,000 \text{ g mol}^{-1} \text{ PDMS})-(2000 \text{ g mol}^{-1} \text{ PCPMS})-(15,000 \text{ g mol}^{-1} \text{ PDMS})$ copolymer in 20 ml toluene.

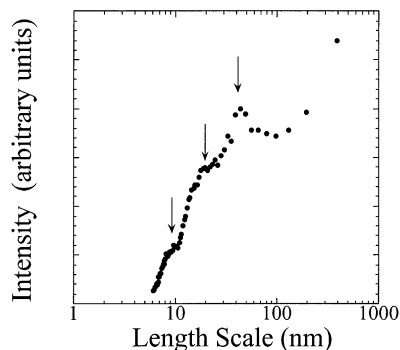


Fig. 11. Radially averaged FFT data of the central TEM image in Fig. 10. The arrows indicate the position of the three characteristic length scales of the image.

3.7. Magnetic properties of the cobalt dispersions

PDMS dispersions with 1.9–6.7 wt% cobalt were prepared. Examples of the magnetic hysteresis curves for samples sealed under inert atmosphere and samples sealed under atmosphere containing air are shown in Fig. 12. The data appear to be a superposition of a saturated magnetic hysteresis curve owing to a mixture of blocked and super-

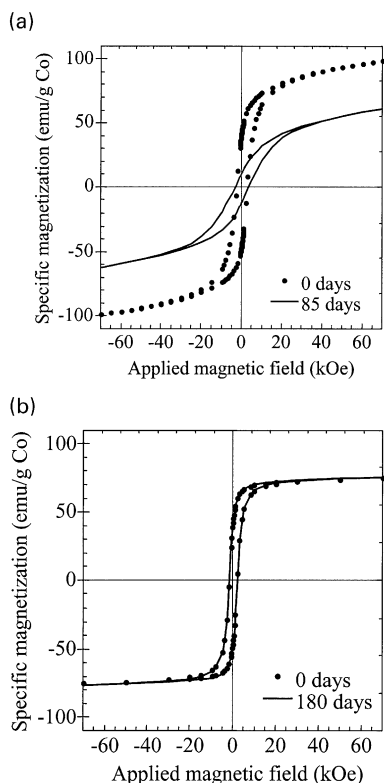


Fig. 12. (a) Hysteresis loops for an air-exposed cobalt nanoparticle dispersion (sample 3) at 5 K after cooling the sample in zero field from room temperature. The loop with the lower specific magnetization values was measured 85 days after the initial loop was recorded. (b) Hysteresis loops for a cobalt nanoparticle dispersion sealed under an argon atmosphere (sample 8) at 5 K after cooling the sample in zero field from room temperature. The two loops were recorded 180 days apart.

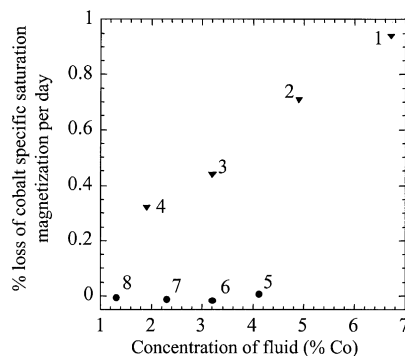


Fig. 13. Loss of cobalt specific saturation magnetization (or cobalt specific magnetization at 70 kOe) per day as a percentage of the original cobalt specific saturation magnetization (or cobalt specific magnetization at 70 kOe); ● samples sealed under argon, ▼ samples sealed with air. The number beside each point corresponds to the sample code in Table 1.

paramagnetic particles and a Brillouin curve owing to the presence of some paramagnetic species. The paramagnetic signal is more apparent in Fig. 12(a) than (b) and results in a continuing rise in specific magnetization even at 70 kOe. The paramagnetic signal may be due to some cobalt carbonyl species which have not been fully reacted. The samples sealed with an air-containing atmosphere were found to have specific magnetizations that were not completely saturated at 70 kOe, presumably because of the presence of paramagnetic species. However, specific magnetizations at 70 kOe were approx 90–110 $\text{emu g}^{-1} \text{Co}$. The samples sealed under inert atmosphere had specific saturation magnetizations of between 58 and 76 $\text{emu g}^{-1} \text{Co}$. Saturation specific magnetization for bulk cobalt is approximately 160 $\text{emu g}^{-1} \text{Co}$ (with very little change between liquid helium temperature and room temperature). Saturation specific magnetizations at room temperature for cobalt nanoparticles in PDMS–PCPMS–PDMS copolymers reported previously [11] were in the range 97–116 $\text{emu g}^{-1} \text{Co}$.

The specific saturation magnetization was also measured at various time intervals to measure the approximate percentage loss of specific saturation magnetization per day. For samples in which the magnetization did not fully saturate at 70 kOe, the specific saturation magnetization was taken to be the specific magnetization at 70 kOe. The specific saturation magnetization of the air-exposed samples decreased over the time period of the experiment (Figs. 12(a) and 13). The rate of specific saturation magnetization loss ranges between 0.3 and 0.9% per day with the most concentrated samples losing the most magnetization per day. This possibly is due to a higher rate of oxygen diffusion in the more concentrated samples. The specific saturation magnetization loss most likely is due to oxidation of the cobalt surface to antiferromagnetic oxides.

Samples sealed under inert gas had no decrease in specific saturation magnetization during the experimental time period (Figs. 12(b) and 13). However, there is evidence for the presence of an oxide layer on the surface of the

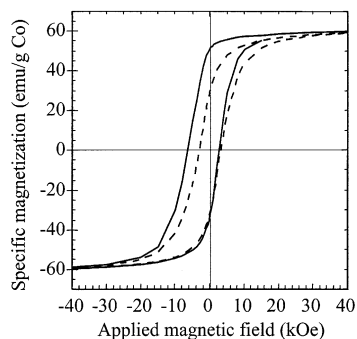


Fig. 14. Hysteresis loops for sample 5 at 5 K after cooling the sample from 220 K in zero field (dashed line) and in a 70 kOe field (solid line).

cobalt particles in the non-air-exposed samples. The shift of the center of the hysteresis loop after cooling in an applied field (Fig. 14) as indicative of exchange anisotropy owing to a layer of antiferromagnetic material, such as cobalt oxide, on the surface of the particle [17,18]. The shift of the field-cooled hysteresis loop was stable for the duration of the experiment. Together with the stable specific saturation magnetization of these samples, this implies that no further oxidation occurred over the experimental time period and supports the idea that oxidation occurred before the start of the magnetization measurements (and probably before being sealed under the argon atmosphere). It is possible that an antiferromagnetic cobalt compound other than cobalt oxide has formed on the particle surface but given the possibility of oxidation of particles during removal of toluene from the reaction fluid, it is most likely that a cobalt oxide layer is formed.

The sensitivity of the magnetic properties of the particles to oxidation implies that the protection of the cobalt surface against oxidation will be a subject of considerable further study. Further analysis of the magnetic properties of these particles will be published at a later date.

4. Conclusions

Well-defined cobalt nanoparticle dispersions with narrow particle size distributions can be prepared in toluene in the presence of PDMS–PCPMS–PDMS triblock copolymer micelles. Each particle is singly coated with a sheath of the block copolymer which may be important for minimizing toxicity issues in biomedical applications. It is hypothesized that this precision in the size and coating integrity in these dispersions is a result of first making the micellar ‘nanoreactors’, then forming the particles inside the intended coating material. Some control of particle size in the 6–10 nm diameter range appears possible by controlling the ratio of the organometallic cobalt precursor to the copolymer during synthesis. This size range may also be important for in vivo applications since there is substantial evidence suggesting that particles in this size range can be

excreted via the renal glomeruli. Ordered self-assemblies of these cobalt particles form spontaneously when the dispersions are cast from toluene. This aspect is not yet understood, but suggests there must be some interparticle attractions–repulsions which control reasonably long-range order.

Magnetic measurements clearly show the decrease in magnetic susceptibility over time for dispersions in contact with an air-containing atmosphere, and this has been attributed to surface oxidation. Protection of the particle surfaces against oxidation, and their detailed characterization is a subject of ongoing study. Magnetic measurements also suggest the presence of an oxide layer around each cobalt particle even when sealed under an inert atmosphere.

Acknowledgements

The authors are grateful for funding from the Orris C. and Beatrice Dewey Hirtzel Memorial Foundation, Carilion Biomedical Institute, the Hamot Health Foundation, the Thomas F. Jeffress and Kate Miller Jeffress Memorial Trust (J-553), and from the Ferrofluidics Corp.

References

- [1] Hess PH, Parker Jr. PH. *J Appl Polym Sci* 1966;10:1915–27.
- [2] Smith TW, Wychick D. *J Phys Chem* 1980;84:1621.
- [3] Wells S. Preparation and properties of ultrafine magnetic particles. PhD Dissertation. Department of Chemistry, University College of North Wales, Bangor. 1989.
- [4] Tannenbaum R. Thermal decomposition of cobalt carbonyl complexes in viscous media. *Inorg Chim Acta* 1994;227:233–40.
- [5] Yin JS, Wang ZL. Preparation of self-assembled cobalt nanocrystal arrays. *Nanostruct Mater* 1999;11(7):845–52.
- [6] Yin JS, Wang ZL. Synthesis of cobalt oxide nanocrystal self-assembled materials. *J Mater Res* 1999;14(2):503–8.
- [7] Petit C, Taleb A, Pileni MP. Cobalt nanosized particles organized in a 2D superlattice: synthesis, characterization and magnetic properties. *J Phys Chem B* 1999;103:1805–10.
- [8] Sun S, Murray CB, Doyle H. Controlled assembly of monodisperse ϵ -cobalt-based nanocrystals. *Mat Res Soc Symp Proc* 1999;577:385–98.
- [9] Platonova OA, Bronstein LM, Solodovnikov SP, Yanovskaya IM, Obolonkova ES, Valetsky PM, Wenz E, Antonietti M. Cobalt nanoparticles in block copolymer micelles: preparation and properties. *Colloid Polym Sci* 1997;275(5):426–31.
- [10] Lin XM, Sorensen CM. Temperature dependence of morphology and magnetic properties of cobalt nanoparticles prepared by an inverse micelle technique. *Langmuir* 1998;14:7140–6.
- [11] Stevenson JP, Rutnakornpituk M, Vadala M, Esker AR, Riffle JS, Charles SW, Wells S, Dailey JP. Magnetic cobalt dispersions in poly (dimethylsiloxane) fluids. *J Magn Magn Mater* 2001;225:47–58.
- [12] Riffle JS, Rutnakornpituk M, Vadala M, Wilson KS, Hoyt J. Synthesis and characterization of novel silicone magnetic materials. *Polym Prepr* 2000;41(2):1368–9.
- [13] Phillips JP, Li C, Dailey JP, Riffle JS. Synthesis of silicone magnetic fluid for use in eye surgery. *J Magn Magn Mater* 1999;194:140–8.
- [14] Weast RC, Lide DR, Astle MJ, Beyer WH. *CRC handbook of chemistry and physics*. Boca Raton: CRC Press, 1989. p. F-37.
- [15] Mahdi SM, Skold RO. Concentration and temperature effects on

- aggregation, clouding and adsorption of a polydisperse non-ionic surfactant in aqueous solution. *Colloid Surf* 1992;66:203–14.
- [16] Alexandridis P, Nivaggioli T, Hatton TA. Temperature effects on structural properties of pluronic P104 and F108 PEO-PPO-PEO block copolymer solutions. *Langmuir* 1995;11:1468–76.
- [17] Bean CP, Meiklejohn WH. New magnetic anisotropy. *Phys Rev* 1956;102:1413–4.
- [18] Nogués J, Schuller IK. Exchange bias. *J Magn Magn Mater* 1999; 192:203–32.